PCCP

Cite this: *Phys. Chem. Chem. Phys.*, 2012, **14**, 11002–11007

www.rsc.org/pccp

**PAPER**

# Reactivity of α-amino-peroxyl radicals and consequences for amine oxidation chemistry†

**Martin T. Schümperli, Ceri Hammond and Ive Hermans***

***Received 8th March 2012, Accepted 11th June 2012***
**DOI: 10.1039/c2cp41306j**



A comparative theoretical study is presented on the formation and fate of α-amino-peroxyl radicals, recently proposed as important intermediates in the aerobic oxidation of amines. After radical abstraction of the weakly bonded αH-atom in the amine substrate, the α-amino-alkyl radical reacts irreversibly with $O_2$, forming the corresponding α-amino-peroxyl radical. $HO_2^{\bullet}$-elimination from various types of α-amino-peroxyl radicals (forming the corresponding imine) and the kinetically competing substrate H-abstraction (forming the α-amino-hydroperoxide) were computationally characterized. Polar solvents were found to reduce the $HO_2^{\bullet}$-elimination barrier, but increase the barrier for H-abstraction. Depending on the reaction conditions (gas or liquid phase, amine concentration, nature of the solvent, and temperature), either of the two mechanisms is favored. The consequences for aerobic amine oxidation chemistry are discussed.

## Introduction

The aerobic oxidation of amines is of considerable technological importance. From a synthetic point of view, amines are viable precursors of valuable chemical building blocks such as imines, nitriles and oximes, amongst others.[1] In addition, amines are also used as absorbers in the post-combustion capture of $CO_2$.[2] However, a severe problem with this technology is the sensitivity of amines to oxidative degradation. Indeed, traces of oxygen in the flue gas cause deterioration of the amine and reduce the efficiency of the scrubber. Despite its importance, the chemistry of aerobic amine oxidations is poorly understood, certainly when compared to alcohol oxidation.

Recently, Suzuki *et al.* investigated the aerobic oxidation of cyclohexylamine to cyclohexanone oxime using a catalytic combination of 1,1-diphenyl-2-picrylhydrazyl (DPPH, a radical mediator) and $WO_3/Al_2O_3$.[3] This one-step reaction is of considerable industrial interest as it provides an alternative route to cyclohexanone oxime, an important polymer building block. It was proposed that DPPH generates the α-amino-cyclohexyl radical upon abstraction of the αH-atom. This C-centered radical is, upon $O_2$-addition, converted to the *c*-$C_6H_{10}(NH_2)OO^{\bullet}$ peroxyl radical (Scheme 1).

The α-amino-cyclohexylperoxyl radical was proposed to abstract an αH-atom and form the α-amino-cyclohexylhydroperoxide (*c*-$C_6H_{10}(NH_2)OOH$). Following its intermediate production, this hydroperoxide was proposed to dehydrate over the heterogeneous catalyst ($WO_3/Al_2O_3$) to the oxime product. However, this mechanism remains speculative as very little is known about α-amino-peroxyl radicals in general. Nevertheless, it is clear that this reaction is radical mediated and achieves an exceptionally high oxime yield of up to 90% which points to very selective radical chemistry.

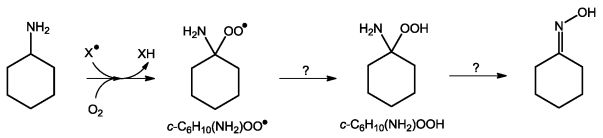


**Scheme 1** Oxidation of cyclohexylamine to cyclohexanone oxime.

In this contribution, the chemistry of α-amino-peroxyl radicals is computationally characterized. In the first part, their formation *via* αH-abstraction from the amine and $O_2$ addition is investigated. Subsequently, we look at the fate of such α-amino-peroxyl radicals. For analogous α-hydroxy-peroxyl radicals, the unimolecular elimination of $HO_2^{\bullet}$ was put forward earlier as a fast reaction, competing with bimolecular H-abstraction.[4] This reaction proceeds *via* an H-bonded intermediate, which rapidly eliminates $HO_2^{\bullet}$ *via* a variational transition state (Scheme 2).[5,6] Depending on the reaction conditions (*e.g.*, *T*, substrate, *etc.*), this $HO_2^{\bullet}$-elimination outruns the competing H-abstraction by the α-hydroxy-peroxyl radical to α-hydroxy hydroperoxide.

The competition between $HO_2^{\bullet}$-elimination, forming an imine, and (α)H-abstraction, forming α-amino-hydroperoxides, for various types of α-amino-peroxyl radicals (see Scheme 3) is therefore investigated, in an attempt to verify or dismiss the

*ETH Zurich, Department of Chemistry and Applied Bio-Sciences, Wolfgang-Pauli-Strasse 10, 8093 Zurich, Switzerland. E-mail: hermans@chem.ethz.ch; Fax: +41 44 6331514; Tel: +41 44 6334258*

† Electronic supplementary information (ESI) available: Cartesian coordinates of important transition states. See DOI: 10.1039/c2cp41306j

 

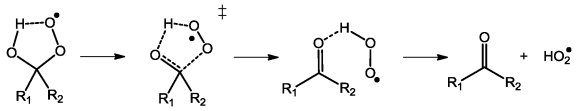

**Scheme 2** $HO_2^{\bullet}$-elimination from a general α-hydroxy-peroxyl radical.

previously hypothesized reaction mechanisms.[7] Unimolecular cleavage of the O–O bond in the peroxyl radical is unimportant in the relevant temperature range, due to the high bond strength.

## Computational methods

All calculations were carried out using the GAUSSIAN09 software package (Revision A.02).[8] Geometries of stationary points (*i.e.* stable intermediates and transition states) were initially optimized at the B3LYP-DFT- or QCISD-level.[9] Subsequently, the relative energies (corrected for zero-point energy – ZPE – differences) were quantitatively refined using various higher levels of theory, such as G3,[10] CBS-QB3,[11] CBS-APNO[12] and G2M[13] (see Table 1). ZPE-corrected relative energies of the stationary points on the Potential Energy Surface (PES) are reported at 0 K.

α-Pinene oxidation experiments were performed at 80 °C in a bubble column reactor at 1 atm $O_2$, as described elsewhere.[14]

## Results and discussion

### Formation of α-amino-peroxyl radicals

Table 2 compares the adiabatic energy barriers for the αH-abstraction from different types of amines by the $CH_3OO^{\bullet}$ radical. Earlier work showed that for analogous H-abstraction reactions from alkanes, alcohols and hydroperoxides, the DFT//DFT results agree within 0.5 kcal $mol^{-1}$ from benchmark methods like G3, CBS-QB3, and G2M//DFT.[4] However, for the abstraction from amines, the various benchmark levels of theory clearly deviate more amongst each other (*i.e.* nearly 2 kcal $mol^{-1}$). Given that those high levels of theory are computationally rather demanding, and that they all have their merits and shortcomings, we prefer to refer to the DFT//DFT results which agree within the range of the benchmark techniques, at a much lower computational cost.

The results in Table 2 show that amines are significantly more prone to αH-abstraction than iso-electronic alcohols. Indeed, the computed barriers for αH-abstraction from methanol, ethanol and iso-propanol by $CH_3OO^{\bullet}$ were previously calculated to be 14.0, 11.8 and 10.3 kcal $mol^{-1}$,[4] respectively; on average more than 3 kcal $mol^{-1}$ higher than for the corresponding amines. This kinetic difference is a direct consequence of the lower αC–H bond strengths in amines than in alcohols (Fig. 1). Notice that the correlation between the abstraction barrier and the αC–H bond (so-called Evans Polanyi correlation) is slightly curved and levels off for weaker αC–H bonds.

The C–H bond strength is inversely proportional to the stability of the radical product. Fig. 2 correlates the H–$CH_2X$ bond strength with the Mulliken spin density on the C-atom in the $^{\bullet}CH_2X$ radical (X = H, $SiH_3$, F, $CH_3$, OH, $NH_2$, $N(H)CH_3$ in order of decreasing H–$CH_2X$ strength). Various parameters influence the stability of the $^{\bullet}CH_2X$ radical, including (when possible) π-back-donation of 2p-orbitals of the substituent X into the half-occupied 2p-orbital on the C-atom,[15] in addition to hyperconjugation and σ-effects. Those combined effects cause the C–H bond strength to decrease in the order $CH_3F$, $CH_3OH$ and $CH_3NH_2$, despite the different substituents being iso-electronic and the electronegativity decreasing in the order F > O > N.

Addition of $O_2$ to the α-amino-alkyl radicals is highly exothermic, with values for $\Delta_r H$ ranging from −27.2 kcal $mol^{-1}$ (CBS-APNO) to −32.5 kcal $mol^{-1}$ ($G2M_{large}$//DFT) for the case of $^{\bullet}CH_2NH_2$, indicating irreversible formation of the α-amino-peroxyl radical.

### Unimolecular $HO_2^{\bullet}$-elimination to imine

Subsequently, the unimolecular decomposition of the α-amino-peroxyl radicals to the corresponding imine plus $HO_2^{\bullet}$ (Reaction 1 in Scheme 3) is investigated. Similar to the analogous reaction of α-hydroxyl-peroxyl radicals (Scheme 2), this reaction is found (*via* intrinsic reaction coordinate analysis) to proceed *via* an H-bonded complex between the imine and $HO_2^{\bullet}$. The break up of this H-bonded complex does not, however, control the overall rate. The rate determining step in the mechanism is the $HO_2^{\bullet}$-elimination, and mainly involves breaking of the C–O bond (see Scheme 4).

Tables 3–5 compare various levels of theory for the decomposition of $^{\bullet}OOCH_2NH_2$, $^{\bullet}OOCHCH_3NH_2$, and $^{\bullet}OOC(CH_3)_2NH_2$, respectively. One observes an excellent agreement (*i.e.*, within 1 kcal $mol^{-1}$) between the CBS-QB3, CBS-APNO and G3 levels of theory. On the other hand, and in contrast to the situation with α-hydroxyl-peroxyl radicals,[5] G2M//DFT gives slightly different results. It seems unlikely that this deviation can be (entirely) attributed to a limited CCSD(T)-basis set,

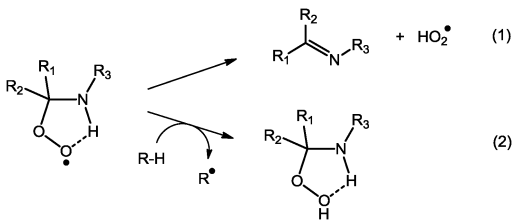

**Scheme 3** Competition between the unimolecular $HO_2^{\bullet}$-elimination (1) and the bimolecular H-abstraction (2) for α-amino-peroxyl radicals.

**Table 1** Summary and details of the levels of theory utilised

| Method | Energy calculation | Geometry optimization and ZPE |
|---|---|---|
| $G2M_{small}$//DFT | E[UCCSD(T)/6-31G(d)] + {E[UMP2/6-311++G(3df,3pd)] − E[UMP2/6-31G(d)]} | UB3LYP/6-311 + G(df,pd) |
| $G2M_{large}$//DFT | E[UCCSD(T)/aug-cc-pVDZ] + {E[UMP2/aug-cc-VTZ] − E[UMP2/aug-cc-pVDZ]} | UB3LYP/aug-cc-pVTZ |
| G2M//QCISD | E[UCCSD(T)/6-311G(df,pd)] + {E[UMP2/6-311++G(3df,3pd)] − E[UMP2/6-311G(df,pd)]} | UQCISD/6-311G(d,p) |
| DFT//DFT | E[UB3LYP/6-311++G(3df,3pd)] | UB3LYP/6-31G(d,p) |

**Table 2** Adiabatic energy barriers (ZPE-corrected; kcal mol$^{-1}$) for the αH-abstraction by $CH_3OO^\bullet$ radicals from various types of amines

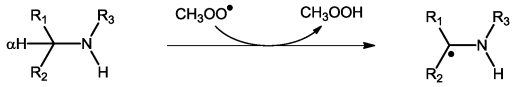


| Amine[a] | CBS-QB3 | G3 | G2M$_{small}$//DFT | G2M$_{large}$//DFT | DFT//DFT |
|---|---|---|---|---|---|
| $R_1 = R_2 = R_3 = H$ | 8.2 | 12.8 | 12.3 | 12.6 | 9.9 |
| $R_1 = R_3 = H$; $R_2 = CH_3$ | 5.9 | 8.0 | 11.1 | 10.5 | 8.5 |
| $R_1 = R_2 = CH_3$; $R_3 = H$ | 4.1 | 6.1 | 9.2 | 9.0 | 7.7 |
| $R_1 = R_2 = H$; $R_3 = CH_3$ | 8.3 | 9.8 | 10.0 | 10.6 | 9.2 |

[a] αC–H bond strengths of the various amines are 89.2, 87.6, 86.0 and 88.5 kcal mol$^{-1}$, respectively, at the B3LYP/6-311++G(d,p) level of theory.

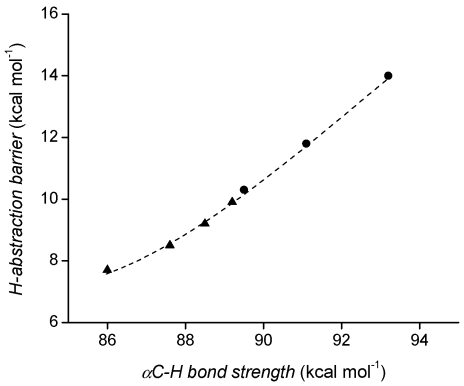


**Fig. 1** Correlation between the computed H-abstraction barrier (DFT//DFT level) and the αC–H bond strength (B3LYP/6-311++G(d,p) level) for various amines (▲) and alcohols (●).

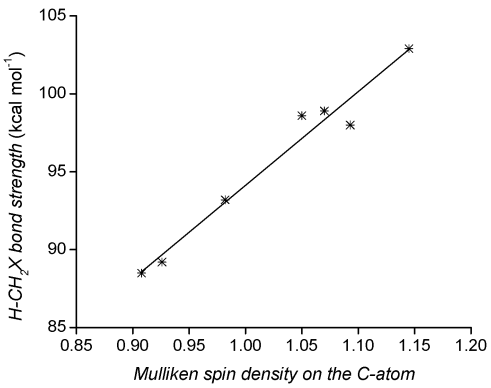


**Fig. 2** Computed H–$CH_2X$ bond strength (B3LYP/6-311++G(d,p) level) *vs.* the Mulliken spin density on the C-atom in the $^\bullet CH_2X$ radical (see the text).

given the close agreement between G2M$_{small}$//DFT and G2M$_{large}$//DFT. More likely, this deviation is due to a slight difference in starting geometry (density-based *vs.* wave-function based methods) for the single-point energy calculations (see Scheme 4). Indeed, the G2M//QCISD results are more in line with the CBS-QB3, CBS-APNO and G3 results. Spin contamination of the wavefunction was found to be negligible ($\langle\langle S^2\rangle\rangle = 0.75 \pm 0.03$ before spin annihilation). In addition, we performed the T1-diagnostic at the UCCSD(T)/6-311++G(df,pd)//QCISD/6-311G(d,p) level of theory for the transition state of the $^\bullet OOCH_2NH_2 \rightarrow CH_2{=}NH + HO_2^\bullet$ reaction. The value obtained (*i.e.* 0.032) is sufficiently small for an open-shell

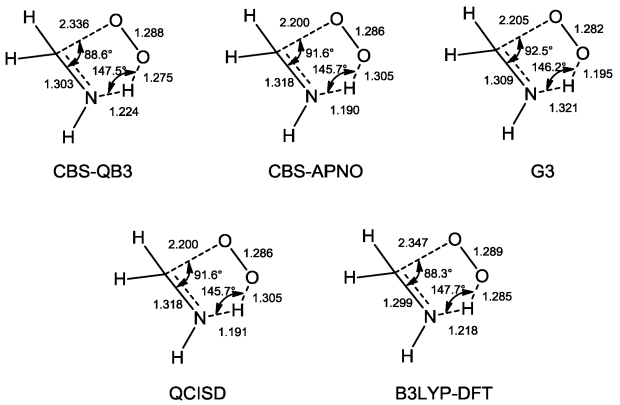


**Scheme 4** Geometry of the transition state for $HO_2^\bullet$-elimination from $^\bullet OOCH_2NH_2$ at various levels of theory (*viz.*, CBS-QB3, CBS-APNO, G3, QCISD/6-311G(d,p) and B3LYP/aug-cc-pVTZ).

doublet structure to neglect multi-reference character. Similar to the situation with α-hydroxy-peroxyl radicals, the DFT//DFT results seem to generate inconsistent errors when compared to the benchmark levels. Functionals which include long-range interactions, such as CAM-B3LYP and wB97, did not, unfortunately, lead to more consistent results.

The endothermicity of $HO_2^\bullet$-elimination from the α-amino-peroxyl is higher than for the corresponding α-hydroxyl-peroxyl cases, in line with the lower stability of >C=N– bonds compared to >C=O bonds. In addition, the activation barriers for the α-amino-peroxyl radicals are found to be nearly 6 kcal mol$^{-1}$ higher than for the corresponding α-hydroxyl-peroxyl radicals. These observations could suggest a slightly later $HO_2^\bullet$-elimination transition state for the amino-systems. This is confirmed upon comparison of the TS structures in Scheme 5: in the case of $CH_2(NH_2)OO^\bullet$, the C···O bond is significantly more elongated, compared to the $CH_2(OH)OO^\bullet$. Nevertheless, the ratio of partition functions (TS over reactant) barely changes, leading to similar pre-exponential factors in the rate constants.

Subsequently, the effect of the $R_3$ substituent (*i.e.*, *N*-alkyl) on the $HO_2^\bullet$-elimination is investigated (Table 6). Apparently substituting a methyl group for an H-atom lowers the endothermicity and the reaction barrier, in line with the higher stability of substituted imines.

In conclusion, $HO_2^\bullet$-elimination from α-amino-peroxyl radicals is slightly more endothermic than for α-hydroxyl-peroxyl radicals, and proceeds with a higher barrier. Alkyl-substituents



 

**Table 3** Relative energies of the characteristic stationary points on the Potential Energy Surface (PES; ZPE-corrected) for the unimolecular decomposition reaction $^{\bullet}OOCH_2NH_2$ $_2NH + HO_2^{\bullet}$

| Stationary point | CBS-QB3 | CBS-APNO | G3 | $G2M_{small}$//DFT | $G2M_{large}$//DFT | G2M//QCISD | DFT//DFT |
|---|---|---|---|---|---|---|---|
| $^{\bullet}OOCH_2NH_2$ | 0.0 | 0.0 | 0.0 | 0.0 | 0.0 | 0.0 | 0.0 |
| TS | 18.6 | 17.4 | 17.9 | 21.9 | 21.4 | 18.5 | 18.6 |
| Complex | 8.5 | 8.4 | 7.6 | 9.5 | 10.1 | 12.8 | 9.8 |
| $CH_2NH + HO_2^{\bullet}$ | 16.7 | 16.8 | 16.0 | 19.9 | 20.6 | 20.9 | 19.1 |

**Table 4** Relative energies of the characteristic stationary points on the Potential Energy Surface (PES; ZPE-corrected) for the unimolecular decomposition reaction $^{\bullet}OOCHCH_3NH_2 \rightleftharpoons CH_3CHNH + HO_2^{\bullet}$

| Stationary point | CBS-QB3 | CBS-APNO | G3 | $G2M_{small}$//DFT | $G2M_{large}$//DFT | DFT//DFT |
|---|---|---|---|---|---|---|
| $^{\bullet}OOCHCH_3NH_2$ | 0.0 | 0.0 | 0.0 | 0.0 | 0.0 | 0.0 |
| TS | 17.7 | 16.5 | 17.1 | 20.7 | 20.7 | 16.2 |
| Complex | 7.8 | 7.6 | 7.2 | 8.7 | 8.3 | 6.7 |
| $CH_3CHNH + HO_2^{\bullet}$ | 17.1 | 16.8 | 16.5 | 19.7 | 20.2 | 16.8 |

**Table 5** Relative energies of the characteristic stationary points on the Potential Energy Surface (PES; ZPE-corrected) for the unimolecular decomposition reaction $^{\bullet}OOC(CH_3)_2NH_2 \rightleftharpoons (CH_3)_2CNH + HO_2^{\bullet}$

| Stationary point | CBS-QB3 | G3 | $G2M_{small}$//DFT | $G2M_{large}$//DFT | DFT//DFT |
|---|---|---|---|---|---|
| $^{\bullet}OOCHCH_3NH_2$ | 0.0 | 0.0 | 0.0 | 0.0 | 0.0 |
| TS | 15.8 | 17.5 | 18.9 | 19.2 | 12.3 |
| Complex | 7.3 | 6.6 | 7.4 | 7.9 | 3.3 |
| $CH_3CHNH + HO_2^{\bullet}$ | 18.2 | 17.6 | 20.2 | 20.8 | 15.2 |

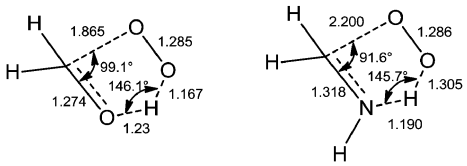


**Scheme 5** CBS-APNO optimized TSs for $HO_2^{\bullet}$-elimination from $CH_2(OH)OO^{\bullet}$ (left) and $CH_2(NH_2)OO^{\bullet}$ (right); distances in Å.

**Table 6** Relative energies of the characteristic stationary points on the Potential Energy Surface (PES; ZPE-corrected) for the unimolecular decomposition reaction $^{\bullet}OOCH_2NHCH_3 \rightleftharpoons CH_2NCH_3 + HO_2^{\bullet}$

| Stationary point | CBS-QB3 | G3 | $G2M_{small}$//DFT | $G2M_{large}$//DFT | DFT//DFT |
|---|---|---|---|---|---|
| $^{\bullet}OOCH_2NHCH_3$ | 0.0 | 0.0 | 0.0 | 0.0 | 0.0 |
| TS | 17.2 | 17.7 | 20.0 | 21.2 | 14.6 |
| Complex | 4.5 | 3.7 | 5.6 | 6.2 | 5.3 |
| $CH_2NCH_3 + HO_2^{\bullet}$ | 13.7 | 13.0 | 16.9 | 17.5 | 15.0 |

on the αC-atom or the N-atom reduce both the energy barrier and the endothermicity of the imine formation.

### H-abstractions: formation of α-amino-hydroperoxides

Competing with the $HO_2^{\bullet}$-elimination is the abstraction of H-atoms from the amine substrate by the α-amino-peroxyl radical (Table 7). Compared to the $HO_2^{\bullet}$-elimination reaction, the barrier of this αH-abstraction reaction is more sensitive to the αC–H bond strength in the corresponding amine substrate (see Fig. 3).

**Table 7** Adiabatic energy barriers (ZPE-corrected; kcal $mol^{-1}$) for the αH-abstraction from different amines at the DFT//DFT level of theory

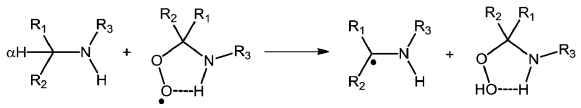


| Amine | DFT//DFT |
|---|---|
| $R_1 = R_2 = R_3 = H$ | 12.0 |
| $R_1 = R_3 = H$; $R_2 = CH_3$ | 10.6 |
| $R_1 = R_2 = CH_3$; $R_3 = H$ | 7.2 |
| $R_1 = R_2 = H$; $R_3 = CH_3$ | 11.1 |

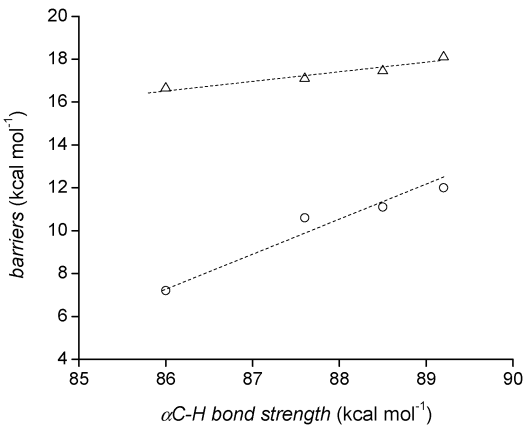


**Fig. 3** Computed barriers for $HO_2^{\bullet}$-elimination (Δ; average of high levels of theory in Tables 3–6) and H-abstraction (○; DFT//DFT level) by α-amino-peroxyl radicals *vs.* αC–H bond strength (B3LYP/6-311++G(d,p)-level) for various amines.

### Solvent effects and quantifying the imine/hydroperoxide branching fraction

All calculations reported so far were modelled in a solvent-free environment (*viz.*, vacuum). As amine oxidations are typically performed in the liquid phase, it remains to be investigated if a solvent could significantly affect the barrier of either of the two reactions. Unfortunately, taking into account all specific solvent interactions is very challenging and certainly beyond routine. The polarisable continuum model (PCM) as implemented in the Gaussian09 software package[8] provides however a convenient and good approximation.[16] This method creates a solute cavity around the species *via* a set of overlapping spheres. Fig. 4 shows the result of such calculations for the barriers of $HO_2^{\bullet}$-elimination and H-abstraction by the $^{\bullet}OOC(CH_3)_2NH_2$ radical at the DFT//DFT level of theory. A list containing all solvents and their dielectric constant ε is given in the ESI.†

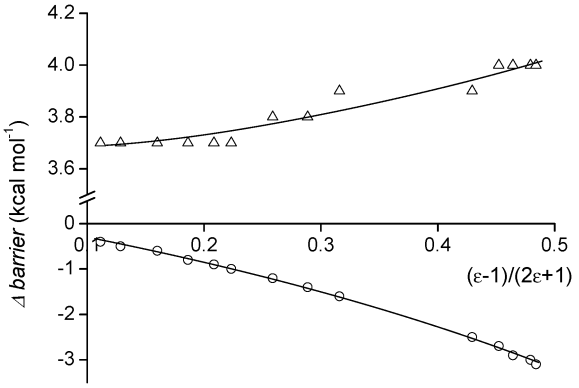


**Fig. 4** Kirkwood plot for the correlation of the changes in activation barrier for $HO_2^{\bullet}$-elimination (○) and bimolecular H-abstraction from $^{i}PrNH_2$ (△) as predicted by PCM-DFT//DFT for $^{\bullet}OOC(CH_3)_2NH_2$.

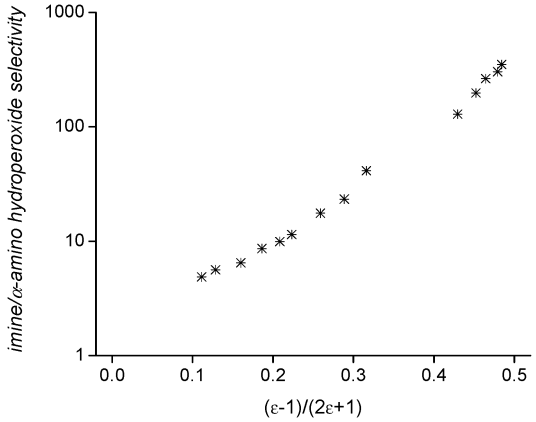


**Fig. 5** Imine/α-amino-hydroperoxide selectivity for the case of isopropylamine at 353 K as a function of $(\varepsilon - 1)/(2\varepsilon + 1)$ (amine concentration is assumed to be 1 M).

It can be observed that solvents with a low to moderate ε-value lower the $HO_2^{\bullet}$-elimination barrier slightly, whereas they significantly increase the barrier of the bimoleculer H-abstraction. This effect should be ascribed to a lower cavity surface of the H-abstraction TS, compared to the separate reactants. For the unimolecular $HO_2^{\bullet}$-elimination, the TS and the α-amino peroxyl reactant have approximately the same available surface, explaining the small influence of non-polar solvents. For more polar solvents, the $HO_2^{\bullet}$-elimination barrier decreases, due to greater stabilization of the transition state than of the α-amino-peroxyl reactant (polarity increase due to C=N bond formation). As the polarity (*viz*., dipole moment) barely changes for the bimolecular H-transfer reaction, this reaction is not as sensitive to the ε-value of the solvent.

The competition between the formation of the imine (*via* $HO_2^{\bullet}$-elimination) and the α-amino-hydroperoxide (*via* bimolecular H-abstraction) can be quantified by eqn (1):

$$\frac{\text{imine}}{\text{hydroperoxide}} = k(\text{imine})/k(\text{abstr})/(\text{amine}) \qquad (1)$$

$k$(imine) and $k$(abstr) in eqn (1) represent the rate constants of channels (1) and (2), respectively, in Scheme 3. Combining the computed barriers with typical pre-exponential factors of $(3 \pm 3) \times 10^{12}$ $s^{-1}$ for $HO_2^{\bullet}$-elimination,[5] and $(3 \pm 2) \times 10^{8}$ $M^{-1}$ $s^{-1}$ for H-abstraction,[17] the imine-to-hydroperoxide ratio can be roughly estimated. Whereas this ratio is predicted to be $\ll 1$ in the absence of a solvent, Fig. 5 shows the evolution of this ratio for the case of isopropylamine at 353 K as a function of the solvent parameter $(\varepsilon - 1)/(2\varepsilon + 1)$, assuming an amine concentration of 1 M (ε being the dielectric constant). It is clear that, according to our predictions, formation of the imine product – as opposed to the hydroperoxide – can be favored by working under dilute conditions in a polar solvent.

It stands to reason that similar iso-branched amines (such as cyclohexylamine) react in a similar manner, and that isopropylamine is indeed a suitable model for such substrates. For instance, at the $G2M_{small}$//DFT level of the theory, the barrier for $HO_2^{\bullet}$-elimination from $c$-$C_6H_{10}(NH_2)OO^{\bullet}$ is predicted to be only 0.7 kcal $mol^{-1}$ higher than for the analogous isopropyl amine system. Moreover, the less complex structure of isopropylamine *vs*. cyclohexylamine allows more reliable levels of theory to be utilized (*vide supra*).

Regarding the experimental work of Suzuki *et al*., dealing with the aerobic oxidation of cyclohexylamine, it should be emphasized that under the reaction conditions employed – *viz*. 353 K, ≈1 M cyclohexylamine in $CH_3CN$ ($\varepsilon$ = 35.7) – cyclohexylimine formation is likely favored over the α-amino-cyclohexylhydroperoxide, in contrast to the original hypothesis. Most likely, the co-produced $HO_2^{\bullet}$ radical is converted to $H_2O_2$ upon a consecutive H-abstraction. Subsequently, $H_2O_2$ can be activated over the $WO_3/Al_2O_3$ catalyst, and epoxidize the imine to an oxazirane (Scheme 6).

*N*-substituted oxaziranes have indeed been synthesized upon the epoxidation of the corresponding imines with peracids.[18] Such *N*-substituted oxaziranes could also be isolated and rearranged to the corresponding amide (lactame; Scheme 7). It seems plausible that under appropriate conditions (such as the presence of a Lewis acid catalyst), the *H*-substituted oxazirane would rearrange to the oxime. We verified this hypothesis experimentally through the addition of *meta*-chloroperoxybenzoic acid (*m*CPBA) to a reaction solution containing cyclohexanone (0.5 M) and aqueous ammonia (0.5 M) in $CH_3CN$ at 353 K. In the presence of $WO_3/Al_2O_3$, cyclohexanone oxime was afforded at approximately 25% yield, in addition to the expected Baeyer–Villiger product (ε-caprolactone). Competing with its epoxidation, cyclohexylimine can also be hydrolyzed by traces of water to yield cyclohexanone; in fact, this is the product which is experimentally obtained in the absence of the $WO_3/Al_2O_3$ catalyst at over 90% selectivity.[3]

Additional evidence supporting our hypothesis of the α-amino-cyclohexylperoxyl radical eliminating $HO_2^{\bullet}$ stems from

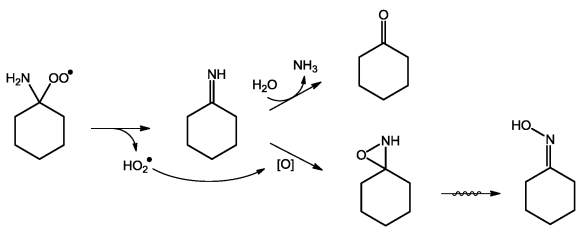


**Scheme 6** Fate of the α-amino-cyclohexylperoxyl radical: formation of imine, which upon epoxidation could lead to the desired oxime product; alternatively, the imine could be hydrolyzed to the ketone.

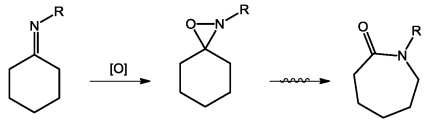


**Scheme 7** Epoxidation of *N*-substituted imine with peracid and the subsequent rearrangement to the lactam.

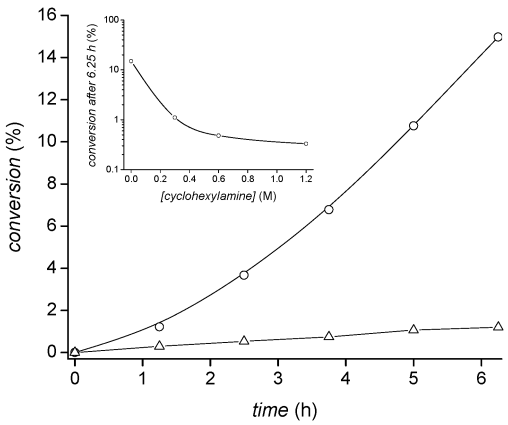


**Fig. 6** Co-oxidation of α-pinene and cyclohexylamine; α-pinene conversion *vs.* time at 80 °C in the absence (○) and presence of 300 mM cyclohexylamine (△); the inset shows the conversion after 6.25 h as a function of the cyclohexylamine concentration.

cyclohexylamine/α-pinene co-oxidation experiments. Fig. 6 shows the rate of conversion of α-pinene at 80 °C *vs.* time in the absence and presence of 300 mM cyclohexylamine. The ratio of $\Delta[\text{amine}]/[\text{amine}]_0$ over $\Delta[\alpha\text{-pinene}]/[\alpha\text{-pinene}]_0$ remains constant at $8 \pm 2$ and corresponds to the ratio of rate constants for radical oxidation. Despite its slightly higher reactivity, the amine clearly inhibits the oxidation of the pinene substrate, whilst barely affecting the selectivity. This observation can readily be understood in terms of $HO_2^\bullet$ radical chemistry: $HO_2^\bullet$ is known to rapidly terminate with the chain-carrying peroxyl radicals (reaction (2)),[19] causing an inhibition of the autoxidation.

$$ROO^\bullet + HO_2^\bullet \rightarrow ROOH + O_2 \qquad (2)$$

## Conclusions

The formation and fate of α-amino-peroxyl radicals has been computationally explored through various quantum-chemical methods. Although iso-electronic with alcohols, it is found that amines are significantly more prone to αH-abstraction. The α-amino alkyl radicals are rapidly converted to α-amino peroxyl radicals, for which two pathways were considered: $HO_2^\bullet$-elimination and bimolecular H-abstraction. Whereas the first channel leads to the formation of an imine, the second channel produces an α-amino hydroperoxide. It was found that the nature of the substituents on both the αC- and the N-atom has an effect on both channels. A significant solvent effect was observed, and was found to steer the selectivity towards $HO_2^\bullet$-elimination. The imine product formed in this manner is believed to yield the desired oxime product under oxidative conditions in the presence of an appropriate Lewis acid catalyst.



## Acknowledgements

The authors thank the ETH Zurich (Grant 17 09-3) for financial support.

## Notes and references

1 M. T. Schümperli, C. Hammond and I. Hermans, *ACS Catal.*, 2012, **2**, 1108.
2 (*a*) Y. Belmabkhout, R. Serna-Guerrero and A. Sayari, *Ind. Eng. Chem. Res.*, 2010, **49**, 359; (*b*) R. Serna-Guerrero, E. Da'na and A. Sayari, *Ind. Eng. Chem. Res.*, 2008, **47**, 9406; (*c*) H. Lepaumier, D. Picq and P.-L. Carrette, *Ind. Eng. Chem. Res.*, 2009, **48**, 9068.
3 K. Suzuki, T. Watanabe and S.-I. Murahashi, *Angew. Chem., Int. Ed.*, 2008, **47**, 2079.
4 I. Hermans, T. L. Nguyen, P. A. Jacobs and J. Peeters, *ChemPhysChem*, 2005, **6**, 637.
5 I. Hermans, J.-F. Müller, T. L. Nguyen, P. A. Jacobs and J. Peeters, *J. Phys. Chem. A*, 2005, **109**, 4303.
6 (*a*) E. M. Evleth, C. F. Melius, M. T. Rayez, J. C. Rayez and W. Forst, *J. Phys. Chem.*, 1993, **97**, 5040; (*b*) S. Olivella, J. M. Bofill and A. Solé, *Chem.–Eur. J.*, 2001, **7**, 3377; (*c*) T. S. Dibble, *Chem. Phys. Lett.*, 2002, **355**, 193; (*d*) J. M. Anglada and V. M. Domingo, *J. Phys. Chem. A*, 2005, **109**, 10786; (*e*) G. da Silva and J. W. Bozzelli, *Chem. Phys. Lett.*, 2009, **483**, 25.
7 G. da Silva, B. B. Kirk, C. Lloyd, A. J. Trevitt and S. J. Blanksby, *J. Phys. Chem. Lett.*, 2012, **3**, 805.
8 M. J. Frisch, G. W. Trucks, H. B. Schlegel, G. E. Scuseria, M. A. Robb, J. R. Cheeseman, G. Scalmani, V. Barone, B. Mennucci, G. A. Petersson, H. Nakatsuji, M. Caricato, X. Li, H. P. Hratchian, A. F. Izmaylov, J. Bloino, G. Zheng, J. L. Sonnenberg, M. Hada, M. Ehara, K. Toyota, R. Fukuda, J. Hasegawa, M. Ishida, T. Nakajima, Y. Honda, O. Kitao, H. Nakai, T. Vreven, J. A. Montgomery, Jr., J. E. Peralta, F. Ogliaro, M. Bearpark, J. J. Heyd, E. Brothers, K. N. Kudin, V. N. Staroverov, R. Kobayashi, J. Normand, K. Raghavachari, A. Rendell, J. C. Burant, S. S. Iyengar, J. Tomasi, M. Cossi, N. Rega, J. M. Millam, M. Klene, J. E. Knox, J. B. Cross, V. Bakken, C. Adamo, J. Jaramillo, R. Gomperts, R. E. Stratmann, O. Yazyev, A. J. Austin, R. Cammi, C. Pomelli, J. Ochterski, R. L. Martin, K. Morokuma, V. G. Zakrzewski, G. A. Voth, P. Salvador, J. J. Dannenberg, S. Dapprich, A. D. Daniels, O. Farkas, J. B. Foresman, J. V. Ortiz, J. Cioslowski and D. J. Fox, *GAUSSIAN 09 (Revision A.2)*, Gaussian, Inc., Wallingford, CT, 2009.
9 (*a*) A. D. Becke, *J. Chem. Phys.*, 1992, **96**, 2155; (*b*) A. D. Becke, *J. Chem. Phys.*, 1992, **97**, 9173; (*c*) A. D. Becke, *J. Chem. Phys.*, 1993, **98**, 5648; (*d*) C. Lee, W. Yang and R. G. Parr, *Phys. Rev. B: Condens. Matter Mater. Phys.*, 1988, **37**, 785.
10 L. A. Curtiss, K. Raghavachari, P. C. Redfern, V. Rassolov and J. A. Pople, *J. Chem. Phys.*, 1998, **109**, 7764.
11 J. A. Montgomery Jr., M. J. Frisch, J. W. Ochterski and G. A. Petersson, *J. Chem. Phys.*, 2000, **112**, 6532.
12 J. W. Ochterski, G. A. Petersson and J. A. Montgomery, *J. Chem. Phys.*, 1996, **104**, 2598.
13 A. M. Mebel, K. Morokuma and M. C. Lin, *J. Chem. Phys.*, 1995, **103**, 7414.
14 (*a*) U. Neuenschwander, F. Guignard and I. Hermans, *ChemSusChem*, 2010, **3**, 75; (*b*) U. Neuenschwander and I. Hermans, *Phys. Chem. Chem. Phys.*, 2010, **12**, 10542.
15 (*a*) T. H. Dunning, W. P. White, R. M. Pitzer and C. W. Mathews, *J. Mol. Spectrosc.*, 1979, **75**, 318; (*b*) J. Peeters, J. Van Hoeymissen, S. Vanhaelemeersch and D. Vermeylen, *J. Phys. Chem.*, 1992, **96**, 1257; (*c*) I. De Boelpaep, B. Vetters and J. Peeters, *J. Phys. Chem. A*, 1997, **101**, 787.
16 J. Tomasi, B. Mennucci and R. Cammi, *Chem. Rev.*, 2005, **105**, 2999.
17 I. Hermans, J. Peeters and P. Jacobs, *J. Org. Chem.*, 2007, **72**, 3057.
18 see *e.g.* (*a*) W. D. Emmons, *J. Am. Chem. Soc.*, 1956, **78**, 6208; (*b*) H. Krimm, K. Hamann and K. Bauer, *US Pat.*, 2,784,182, 1957; (*c*) W. D. Emmons, *J. Am. Chem. Soc.*, 1957, **79**, 5739.
19 D. M. Rowley, R. Lesclaux, P. D. Lightfoot, B. Nozière, T. J. Wallington and M. D. Hurley, *J. Phys. Chem.*, 1992, **96**, 4889.